Full Length Research Paper

Effect of substrate temperature on physical properties of In$_2$O$_3$:Sn films deposited by e-beam technique

H. A. Mohamed[1,2]

Physics Department, Faculty of Science, Sohag University, 82524 Sohag, Egypt.
Science Department, Physics Teachers College, King Saud University, 11148 Riyadh, KSA.
E-mail: hussein_abdelhafez2000@yahoo.com. Tel: +966-1-4046666 or +966-1-4046666. Fax: +966-1-4050477.

Indium tin oxide (ITO) thin films were prepared by electron beam evaporation at different substrate temperatures. The structural studies were carried out by X-ray diffraction. Optical properties of the films were studied in the ultraviolet-visible-near infrared (UV-Vis-NIR) region (200 to 2500 nm). Electrical studies were carried out at room temperature of ITO films. The results showed that with increase in substrate temperature, the optical transmittance gradually increased up to 93% in the visible region, the transmittance edge gradually shifted to short wavelength and the corresponding refractive index and thermal emissivity decreased. The structure of ITO films was polycrystalline and the crystallinity was improved with increasing substrate temperature. The electrical resistivity decreased and attained its minimum value of 5.2 × 10^{-4} Ω cm at 300°C.

Key words: Thin films, electron beam; indium tin oxide (ITO), optical constants, electrical properties, structure properties.

INTRODUCTION

Transparent conducting oxides (TCOs) are used widely as electrodes due to their high transmittance of visible light wavelengths and high electrical conductivity (Minami, 2005; Peelaers et al., 2012; Ramesh et al., 2012). They are used as electrodes in various applications, such as photovoltaic solar cells, liquid crystal displays, sensors and organic light emitting devices (Xue et al., 2004; Chou et al., 2009; Müller et al., 2003). Among the existing TCOs, indium tin oxide (ITO) is one of the most frequently used materials, because of its unique characteristics, such as good conductivity, high optical transmittance over the visible wavelength region and excellent adhesion to substrates. Photochemical properties, which originate from its n-type highly degenerate semiconductor behavior along with a wide band gap, are other advantages of ITO films (Fallaha et al., 2006; Choi et al., 2003; Huang et al., 2004; Chen et al., 2004). It is also well known that the electrical and optical properties of semiconducting oxides like In$_2$O$_3$ depend strongly on defect density created by external doping or disturbed stoichiometry as well as their preparation and growth conditions. In order to obtain optimal characteristics, that is, high transparency in visible region and high conductivity at room temperature, parameters such as film thickness, dopant type and its amount, annealing temperature, deposition conditions and heat treatment have to be optimized (Fallah et al., 2010).

This article presents an investigation on the effect of substrate temperature on the optical, electrical and microstructural properties of the ITO thin film grown on glass substrate by electron beam evaporation technique. The electron beam evaporation technique provides an economical and efficient use of evaporant, since it offers the following advantages: (1) it has a high power density, and hence a wide range of control over evaporation rates, (2) it is used to evaporate materials which have a high melting point (Ali et al., 2005).

EXPERIMENTAL TECHNIQUE

In the present study, indium tin oxide films were deposited by electron beam evaporation technique of ITO target containing 90 wt% of In$_2$O$_3$ and 10 wt% of SnO$_2$. The used target was prepared from In$_2$O$_3$ (99.99% pure) and SnO$_2$ (99.999% pure) powders. To increase complete mixing, the mixtures were grinded for at least 3

h. Then, they were made in tablet form using a cold pressing technique and then sintered at 1000°C for 5 h in air. Edward's high vacuum coating unit model E306A under pressure of 5×10^{-5} Torr during film deposition was used to prepare ITO films onto ultrasonically cleaned glass slides of dimension 2.5 × 1 cm. The film thickness (~140 nm) and deposition rate were controlled by means of a digital film thickness monitor model TM200 Maxtek. The structural characterization of the films were carried out using Phillips (PW-1710) $Cu\text{-}k_\alpha$ diffractometer (λ= 1.541838 Å) by varying diffraction angle 2θ from 4 to 80° by step width of 0.04. The transmittance (T) and reflection (R) data were measured using a Jasco V-570 ultraviolet-visible-near infrared (UV-Vis-NIR) spectrophotometer in the wavelength range from 200 to 2500 nm at normal incidence. The optical parameters, namely optical energy gap (E_g), free carrier concentration (N), refractive index (n), extinction coefficient (k), real and imaginary dielectric constants (ε', ε''), optical resistivity (ρ_{opt}), packing density (P) and relaxation time (τ) were calculated using the two aforementioned quantities (T and R). The measurements of electrical properties of ITO films were performed by means of a digital Keithley 614 electrometer using two-probe technique. Electrical contacts were made by applying silver paste over the surface of the films with a separation of 3 mm. In the following parts of this article, the term "as-deposited films" means films deposited at room temperature.

RESULTS AND DISCUSSION

Film structure

X-ray diffraction spectra were used to examine the structure of indium tin oxide films deposited at different values of substrate temperature (as-deposited, 150, 250 and 350°C) using electron beam evaporation technique. The results of X-ray analysis are as shown in Figure 1. The analysis of the crystal structure was revealed to some peaks. The clearest peaks appeared at 2θ values 30.52 and 50.13, were due to reflections from 222 and 441 planes of ITO, respectively. The peak intensity of the 222 plane was predominant among the other reflection planes indicating the preferential orientation of the ITO film. The X-ray analysis of as-deposited ITO films is partially amorphous as reported (Ali et al., 2005; El Amrani et al., 2010; Lee, 2004; Lee and Park, 2004). The major peaks due to SnO_2 at 26.5°C and SnO at 33.2°C were absent in the observed pattern, indicating complete miscibility of In and Sn in the proposed composition (Sujatha et al., 2002). Nisha et al. (2005) reported that with increasing the substrate temperature above 100°C, an increase of 222 peak was observed of ITO films deposited by radio frequency (RF) magnetron sputtering. The grain size of the ITO film was calculated from the line broadening of the 222 diffraction line according to the Scherrer equation.

$$D = \frac{0.9\,\lambda}{\beta \cos\theta} \qquad (1)$$

where λ is the wavelength of the X-ray radiation and β is the diffraction broadening of the peak at half-height for a
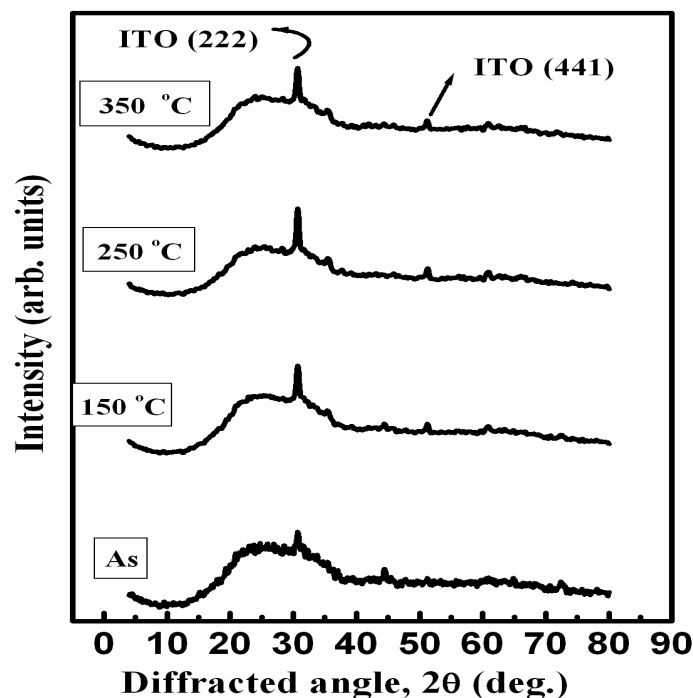
Figure 1. X-ray diffraction of ITO films prepared at different substrate temperatures.

Bragg's angle θ. Values of grain size along 222 plan of indium tin oxide films at different substrate temperatures were calculated and listed in Table 1. From this table, it is clear that the variation of grain size with substrate temperature is not big and the maximum value of 20 nm was observed for films deposited at substrate temperature of 250°C whereas the full width at half maximum (FWHM) records its minimum value as shown in Table 1. In general we can conclude that the substrate temperature leads to the enhancement of the film crystallinity.

Optical and electrical properties

Figure 2 shows the transmission spectra of ITO films deposited at various substrate temperatures. It is clear that the films deposited at room temperature and at low values of substrate temperatures (150 and 200°C) represent low transmission in the visible and near infrared region of the electromagnetic spectrum. The low transmission may be due to a lack of oxygen during deposition by electron beam technique, which leads increase in the oxygen deficiency (Ali et al., 2005; Chopra et al., 1983) which decreases the optical transmittance. Moreover, according to Nisha et al. (2005), low transmission in NIR region is due to high free carrier concentration. Therefore, higher carrier concentration results in higher reflection in long wavelength region as
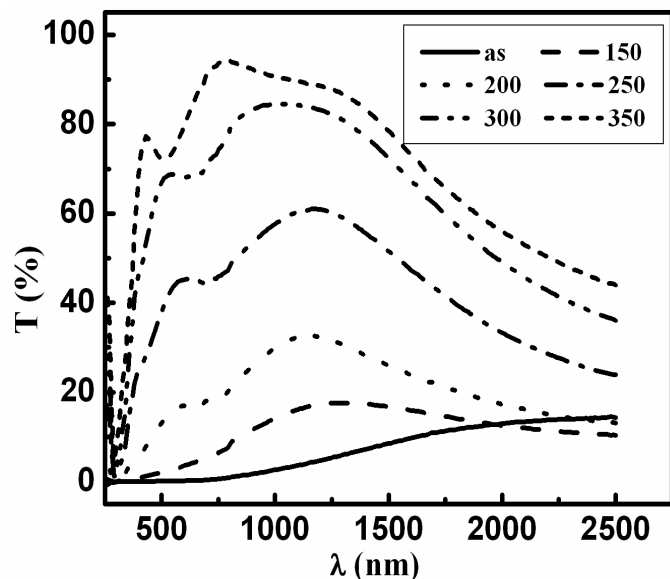
Figure 2. Optical transmittance spectra (T%) of ITO films as a function of wavelength (λ) with variation of substrate temperature.
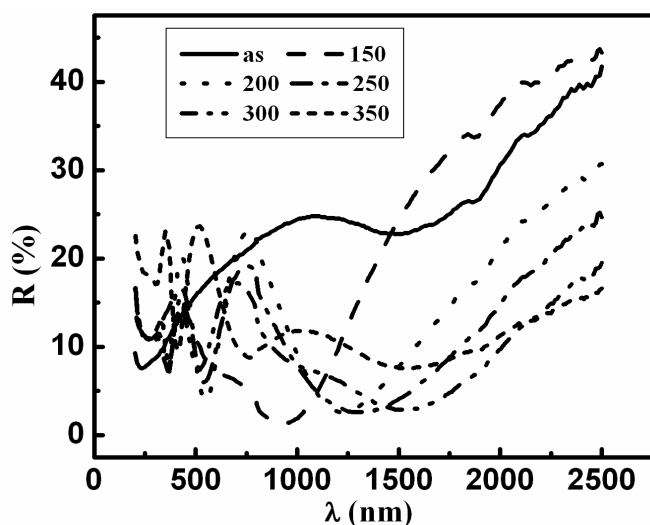
Figure 3. Optical reflection spectra (R%) of ITO films as a function of wavelength (λ) with variation of substrate temperature.

seen in the dependence of reflection spectra on wavelength (Figure 3). As increase in substrate temperature above 250°C, a significant increase in the film transmission can be observed. The highest transmission of 93% at wavelength 700 nm was observed for ITO films prepared at substrate temperature of 350°C. the increase of the film transparency maybe due to decrease in oxygen deficiency as well as enhancement of the film crystallinity with increase the substrate temperature.

The optical band gap of the films were determined by extrapolating the linear portion of the hv versus $(\alpha hv)^2$ curve to $(\alpha hv) = 0$ as shown in Figure 4a. The absorption coefficient α was calculated from the transmittance T and reflection R data using the equation (Mohamed, 2007):

$$\alpha = \frac{2.303}{d} \log_{10}\left(\frac{1-R}{T}\right) \qquad (2)$$

where d is the film thickness. From Figure 4a, it is clear that the ITO films directly allowed transitions. Figure 4b shows the dependence of transmission on estimated optical band gap of ITO film at different values of substrate temperature. It is noted that films prepared at low substrate temperature represent low band gap and hence transmission. This maybe correlated to high carrier concentration (Figure 8). However, at high carrier concentrations, the band gap is narrowing due to electron-electron scattering and electron-impurity scattering. Besides, the energy gap increases with further increase of substrate temperature associated with shift in the absorption edge to lower wavelength as shown in Figure 2. Films deposited at substrate temperatures of 350°C show the highest optical energy gap of 3.45 eV. This behaviour of band gap at high temperature maybe due to improvement of film crystallinity and decrease in the oxygen deficiency. As shown in Figure 4b, it could directly combine the function of transmittance and energy band gap. It is clear that the transmittance in the visible region (in which the solar spectrum is maximum) increases with increase in the optical energy band.

Using the transmission and reflection spectra (Tauc, 1979), the spectral refractive index (n) and extinction coefficient (K) of ITO films were estimated at different substrate temperatures. From Table 1, we can see that the refractive index decreases with the increase of the substrate temperature. This may be attributed to the variation of the packing density. The refractive index data are indicative of the film packing density (Cho and Hwangbo, 1996; Shen et at., 2007). The relation between refractive index n and packing density p can be illustrated by:

$$n = P n_s + (1-P) n_v \qquad (3)$$

where n_s and n_v are the refractive index of the solid part of the film (single crystal value) and the voids, respectively. Using the aforementioned relation, the packing densities for ITO films deposited at different substrate temperatures are determined and listed in Table 1. The value of the refractive index for the single crystal ($n_s = 2.19$) was taken from Kim et al. (2008). It can be seen that the packing density value of ITO films deposited at low substrate temperature is closed to unity, that is, closed to those of single crystal. Decrease in
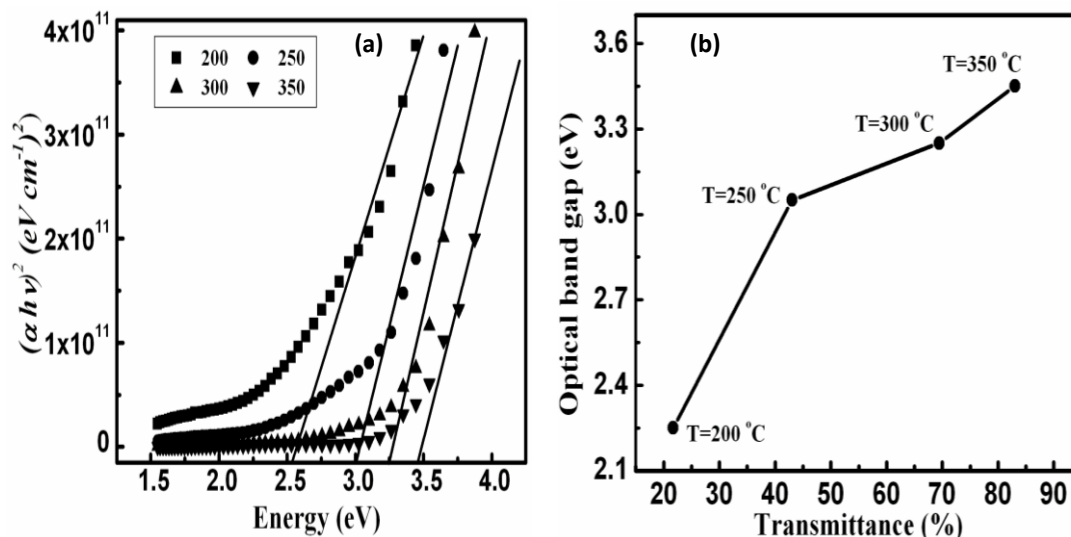
Figure 4. Plots of $(\alpha h v)^2$ versus photon energy (hv) (a), the average transmittance values of ITO film in the visible region as a function of energy band gap (b) at various values of substrate temperature.
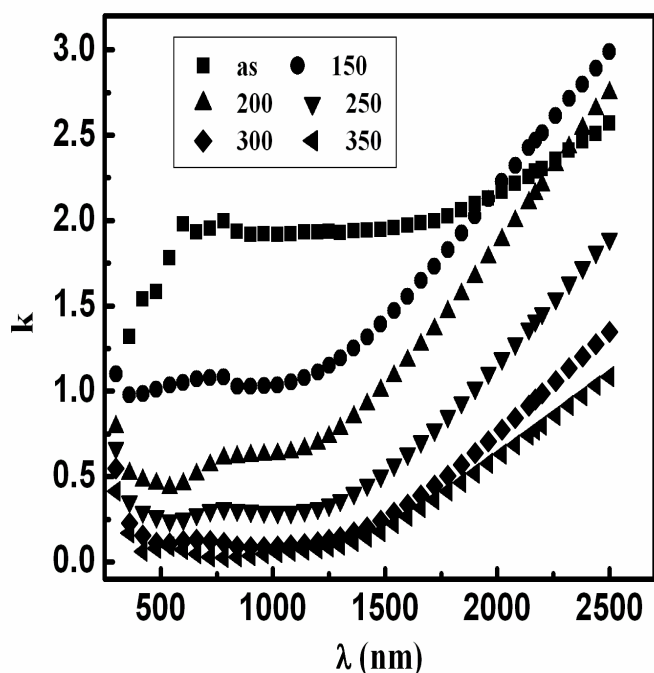
Figure 5. Variation of extinction coefficient (k) with wavelength (λ) at different values of substrate temperature.

packing density with increase in the substrate temperature is correlated to increase in grain size as reported by Shen et al. (2007) (Figure 2). On the other hand, the variation of extinction coefficient (k) with wavelength (λ) of ITO films at different substrate temperatures is as shown in Figure 5. The extinction coefficient of ITO thin films deposited at room

temperature and low substrate temperatures are large, then extinction coefficient decreases with the increase of temperature and becomes very small at substrate temperature of 350°C particular in the visible region. The factors that contributed in increasing the film transmission with substrate temperature are considered the same factors that lead to decrease in the extinction coefficient. Therefore the extinction coefficient is inversely proportion with transmission.

One of valuable applications of indium tin oxide, namely, transparent heat mirror coatings (low thermal emissivity) have attracted increased interest in reducing heat radiation loss through window panes from ecological and sustainable aspects (De et al., 2007). The thermal emissivity was calculated using the following equation (Biswas et al., 2003) and plotted as shown in Figure 6.

$$\varepsilon = 1 - R_{IR} - T_{IR} \quad (4)$$

where R_{IR} and T_{IR} is the average reflection and transmission in the near infrared region. In this figure, the first data point (zero) corresponds to as-deposited films. As shown in this figure, for as-deposited ITO films and at low substrate temperature, the thermal emissivity records high value of 0.7. This is due to the increase of free carrier concentrations, which lead to increase in the probability of carrier-carrier and carrier-photon interaction. The later process results in increase in the reflection in near infrared region as shown in Figure 3. With further increase in substrate temperature, the values of thermal emissivity start to decrease and attain their minimum value of 0.041 at 350°C. This can be explained
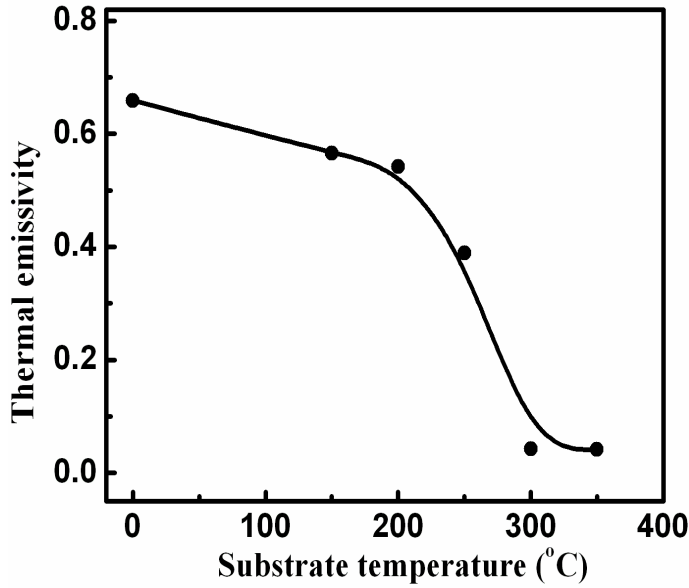
Figure 6. The substrate temperature dependence of the thermal emissivity of ITO films.

by enhancement of the film crystallinity, suggesting that there is an increase in carrier mobility, and thus, the conductivity of the film is enhanced (Fangli et al., 2010).

Figure 7 shows the variations of real ε' (Figure 7a) and imaginary ε'' (Figure 7b) dielectric constant with λ^2 and λ^3, respectively, at different values of substrate temperature. The aforementioned two optical constant were calculated using the following equations (Saadeddin et al., 2007):

$$\varepsilon' = n^2 - k^2 = \varepsilon_\infty - \frac{e^2}{4\pi^2 c^2 \varepsilon_0}\left(\frac{N}{m^*}\right)\lambda^2 \quad (5)$$

$$\varepsilon'' = 2nk = \frac{e^2}{4\pi^3 c^3 \varepsilon_0}\left(\frac{N}{m^*}\right)\frac{1}{\tau}\lambda^3 \quad (6)$$

where n is the refractive index, k is the extinction coefficient, ε_∞ is the high frequency permittivity, e is the electron charge, c is the light velocity, ε_0 is the permittivity of free space, m^* is the electron effective mass ($m^* = 0.4\ m_0$) (Solieman and Aegerter, 2006), τ is the relaxation time and λ is the incident wavelength. From this figure, it is evident that both ε' and ε'' linearly vary with λ^2 and λ^3, respectively, suggesting that they obey the free electron Drude model. The estimated values of free carrier concentration (from Figure 7a and Equation 5) and relaxation time (from Figure 7b and Equation 6) were plotted as a function of substrate temperature in Figure 8. It can be noted that, the free carrier concentration rapidly

decreases at low values of substrate temperature and slowly decreases at high temperatures. But in general, the free carrier concentration has high values of 10^{20} cm^{-3} all over the ranges of substrate temperature. The high values of N may be due to oxygen vacancies and the replacement of In^{3+} by Sn^{4+} (Yamaguchia et al., 2004). In addition, as reported by Tahar et al. (1998) that, ITO thin film is a high degenerated n-type semiconductor with high electron carrier concentration caused by the overlap of the Fermi level with the conduction level at the bottom of the conduction band. The film degeneracy is confirmed by evaluating Fermi energy using relation (Babar et al., 2010):

$$\Delta E = \left(\frac{h^2}{8m^*}\right)\left(\frac{3N}{\pi}\right)^{2/3} \quad (7)$$

where h is the Plank's constant. The calculated value of Fermi energy lies in the range of 0.332 to 0.243 eV (Table 1). It is clear that the Fermi energy values are higher comparison in kT value at room temperature which is the evidence for degenerated nature of ITO material.

The behaviour of variation of relaxation time with substrate temperature is similar to the variations of carrier mobility (μ) and mean free path (L) which were calculated (Ali et al., 2006) and plotted as shown in Figure 9. Increase in carrier mobility with substrate temperature up to 250°C is correlated to enhance the film ordering. Besides, the mean free path values of as-deposited films and films deposited at low substrate temperature are considered shorter than their corresponding grain size (Table 1). Therefore, the mobility is limited by the ionized impurity scattering. At high substrate temperature, the mean free path values are in the same range of grain size, therefore, the mobility is limited by the grain boundary scattering (Babar et al., 2010).

According to the earlier explanation of mobility, mean free path and relaxation time, it is expected that the electrical resistivity (ρ) decreases with increase in the substrate temperature as shown in Figure 10. The minimum value of resistivity (5.2×10^{-4} Ωcm) is observed at substrate temperature of 300°C. Increase in electrical resistivity at high substrate temperature maybe due to the decrease in free carrier concentration as shown in Figure 8. Moreover, the optical resistivity was calculated using the following equation and plotted as shown in Figure 10 as a function of substrate temperature.

$$\rho_{opt} = \frac{1}{\varepsilon_\infty \varepsilon_0 \omega_P^2 \tau} \quad (8)$$

$$\omega_P = \left(\frac{Ne^2}{\varepsilon_0 \varepsilon_\infty m^*}\right)^{1/2} \quad (9)$$
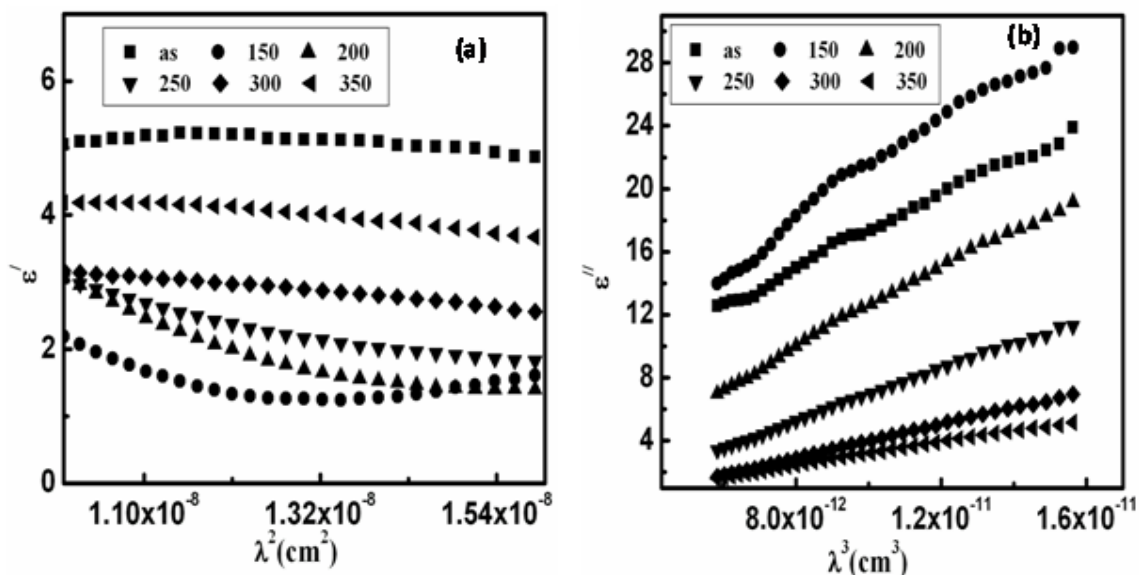
Figure 7. Variations of real ε′ (a) and imaginary ε″ (b) dielectric constant with λ^2 and λ^3, respectively, at different values of substrate temperature.
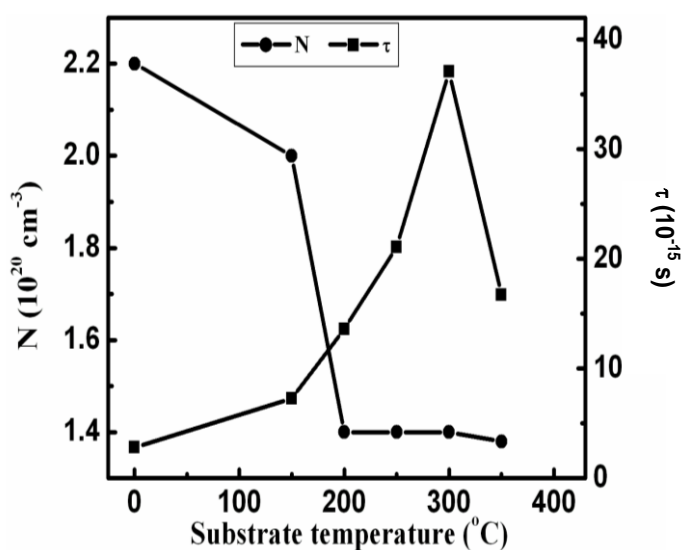
Figure 8. Plots of the free carrier concentration (N) and relaxation time (τ) for ITO films at different values of substrate temperature.

Table 1. Variations of grain size (D), full width at half maximum (FWHM), refractive index (n), packing density (P), and Fermi energy (ΔE) with substrate temperatures (T_s) of indium tin oxide films.

T_s (°C)	D (nm)	FWHM	n	P	ΔE
as	-	-	2.79	-	0.332
150	17.7	0.466	2.29	1.1	0.321
200	-	-	2.28	0.89	0.246
250	20.1	0.411	2.03	0.85	0.246
300	-	-	1.89	0.74	0.246
350	17.9	0.460	1.87	0.72	0.243
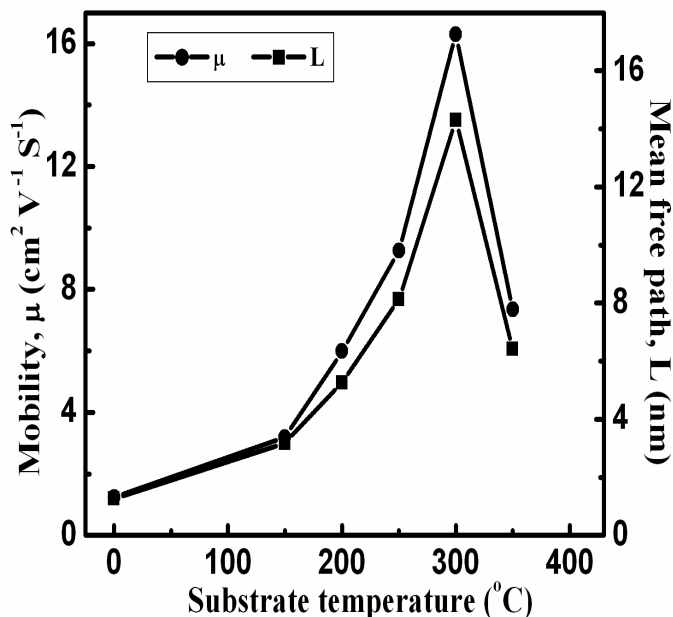
Figure 9. Carrier mobility (μ) and mean free path (L) dependence of substrate temperature of ITO films.
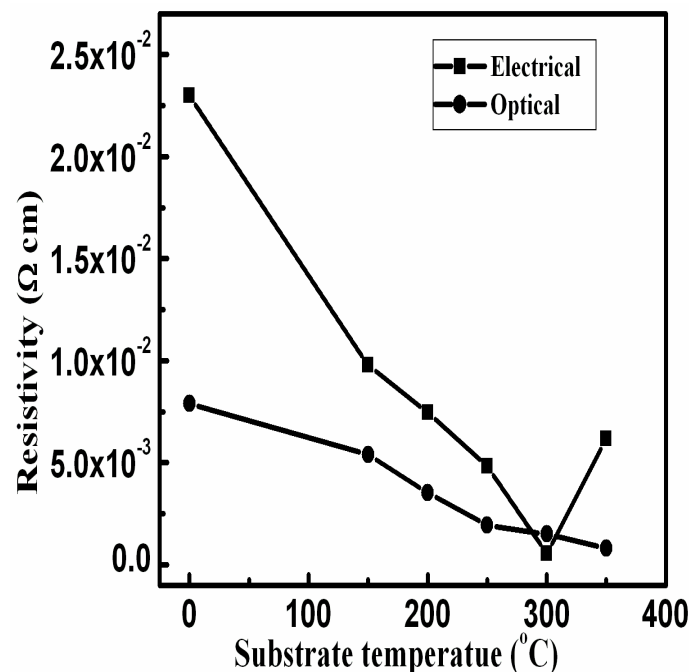
Figure 10. Variations of the electrical and optical resistivity with substrate temperature.

where ω_P is the plasma frequency. The optical resistivity has the same trends of electrical resistivity and its values are mostly lower than electrical resistivity all over the range of substrate temperature as observed in other work

(Ali et al., 2007; Mohamed, 2009).

Conclusions

The effect of substrate temperature on structural, optical and electrical properties of ITO thin film prepared by electron beam evaporation was studied in this work. From the obtained results it was concluded that with increase in the substrate temperature:

1) The crystallinity was improved and the average grain size was about 20 nm.
2) ITO represented direct optical gap that increased up to 3.45 eV with increase in the substrate temperature to 350°C and the corresponding transmittance was about 93% in the visible region.
3) The electrical resistivity was decreasing and attained its minimum value at 300°C.
4) The free carrier concentration, refractive index, packing density, extinction coefficient and thermal emissivity was decreasing.
5) The variation of both electrical and optical resistivity with substrate temperature can be explained in terms of the behaviour of mean free path, relaxation time and carrier mobility.
6) The mobility was limited by the ionized impurity scattering at low substrate temperature and by the grain boundary scattering at high substrate temperature.
7) ITO films were degenerate n-type and their degeneracy decreased since the calculated value of Fermi energy which lied in the range of 0.332 to 0.243 eV recorded value that is greater than *kT* value at room temperature.

According to these promising results and under these experimental conditions, ITO films can be used in various optoelectronic applications, such as photovoltaic solar cells, liquid crystal displays and transparent heat mirror coatings.

REFERENCES

Ali HM, Mohamed HA, Mohamed SH (2005). Enhancement of the optical and electrical properties of ITO thin films deposited by electron beam evaporation technique. Eur. Phys. J. Appl. Phys., 31: 87-93.
Ali HM, Abd El-Raheem MM, Megahed NM, Mohamed HA (2006). Optimization of the optical and electrical properties of electron beam evaporated aluminum-doped zinc oxide films for opto-electronic applications. J. Phys. Chem. Solids, 67: 1823-1829.
Ali HM, Mohamed HA, Wakkad MM, Hasaneen MF (2007). Properties

of transparent conducting oxides formed from CdO alloyed with In_2O_3. Thin Solid Films, 515: 3024-3029.

Babar AR, Shinde SS, Moholkar AV, Bhosale CH, Kim JH, Rajpure KY (2010). Structural and optoelectronic properties of antimony incorporated tin oxide thin films. J Alloy Compd., 505: 416- 422.

Biswas PK, De A, Pramanika NC, Chakraborty PK, Ortner K, Hock V, Korder S (2003). Effects of tin on IR reflectivity, thermal emissivity, Hall mobility and plasma wavelength of sol–gel indium tin oxide films on glass. Mater. Lett., 57: 2326-2332.

Chen BJ, Sun XW, Tay BK. (2004). Fabrication of ITO thin films by filtered cathodic vacuum arc deposition. Mater. Sci. Eng. B., 106: 300-304.

Cho HJ, Hwangbo CK (1996). Optical inhomogeneity and microstructure of ZrO_2 thin films prepared by ion-assisted deposition. Appl. Opt., 35: 5545- 5552.

Choi JB, Kim JH, Jeon KA, Lee SY (2003). Properties of ITO films on glass fabricated by pulsed laser deposition. Mater. Sci. Eng., B., 102: 376-379.

Chopra KL, Major S, Pandya DK (1983).Tansparent conductors – A status review. Thin Solid Films, 102: 1-46.

Chou TH, Cheng KY, Chang TL, Ting CJ, Hsu HC, Wu CJ, Tsai JH, Huang TY (2009). Fabrication of antireflection structure on TCO film for reflective liquid crystal display, Microelectron. Eng., 86: 628-831.

De A, Biswas PK, Manara J (2007). Study of annealing time on sol-gel indium tin oxide films on glass. Mater. Charact., 58: 629- 636.

El Amrani A, Hijazi F, Lucas B, Bouclé J, Aldissi M (2010). Electronic transport and optical properties of thin oxide films. Thin Solid Films, 518: 4582- 4585.

Fallaha HR, Ghasemia M, Hassanzadehb A, Stekic H (2006). The effect of deposition rate on electrical, optical and structural properties of tin-doped indium oxide (ITO) films on glass at low substrate temperature. Physica B., 373: 274- 279.

Fallah HR, Varnamkhasti MG, Vahid MJ (2010). Substrate temperature effect on transparent heat reflecting nanocrystalline ITO films prepared by electron beam evaporation. Renew. Energy, 35: 1527-1530.

Fangli DU, Ning W, Dongmei Z, Yingzhong S (2010). Preparation, characterization and infrared emissivity study of Ce-doped ZnO films. J. Rare Earth, 28: 391-395.

Huang CJ, Su YK, Wu SL (2004). The effect of solvent on the etching of ITO electrode. Mater. Chem. Phys., 84: 146-150.

Kim JK, Chhajed S, Schubert MF, Schubert EF, Fischer AJ, Crawford MH, Cho J, Kim H, Sone C (2008). Light-Extraction Enhancement of GaInN Light-Emitting Diodes by Graded-Refractive-Index Indium Tin Oxide Anti-Reflection Contact. Adv. Mater., 20: 801-804.

Lee HC (2006). Electron scattering mechanisms in indium-tin-oxide thin films prepared at the various process conditions. Appl. Surf. Sci., 252: 3428-3435.

Lee HC, Park OO (2004). Electron scattering mechanisms in indium-tin-oxide thin films: Grain boundary and ionized impurity scattering. Vacuum, 75: 275-282.

Minami T (2005). Transparent conducting oxide semiconductors for transparent electrodes. Semicond. Sci. Technol., 20: S35-S44.

Mohamed HA (2007). The effect of annealing and ZnO dopant on the optoelectronic properties of ITO thin films. J. Phys. D: Appl. Phys., 40: 4234-4240.

Mohamed HA (2009). Structure and optical constants of electron beam deposited zinc nitride films. Eur. Phys. J. Appl. Phys., 48: 20504P1-P6.

Müller CD, Falcou A, Reckefuss N, Rojahn M, Wiederhirn V, Rudati P, Frohne H, Nuyken O, Becker H, Meerholz K (2003). Multi-colour organic light-emitting displays by solution processing. Nature, 421: 829-833.

Nisha M, Anusha S, Antony A, Manoj R, Jayaraj MK (2005). Effect of substrate temperature on the growth of ITO thin films. Appl. Surf. Sci., 252: 1430-1435.

Peelaers H, Kioupakis E, Van de Walle CG (2012). Fundamental limits on optical transparency of transparent conducting oxides: Free-carrier absorption in SnO_2. Appl. Phys. Lett., 100: 011914- 011916.

Ramesh MK, Timothy CH, Daniel K, George W, Adrián MT, Kyle B, Krishna CM (2012). Characterization of transparent conducting oxide thin films deposited on ceramic substrates. Mater. Lett., 66: 233-235.

Saadeddin I, Pecquenard B, Manaud JP, Decourta R, Labruge`re C, Buffeteau T, Campet G (2007). Synthesis and characterization of single- and co-doped SnO_2 thin films for optoelectronic applications. Appl. Surf. Sci., 253: 5240-5249.

Shen Y , Shao S, Yu H, Fan Z, He H, Shao J (2007). Influences of oxygen partial pressure on structure and related properties of ZrO_2 thin films prepared by electron beam evaporation deposition. Appl. Surf. Sci., 254: 552- 556.

Solieman A, Aegerter MA (2006). Modeling of optical and electrical properties of In_2O_3 : Sn coatings made by various techniques, Thin Solid Films, 502: 205-211.

Sujatha P, Chatterjee M, Ganguli D (2002). Indium tin oxide nano-particles through an emulsion technique. Mater. Lett., 55: 205-210.

Tahar RBH, Ban T, Ohya Y, Takahashi Y (1898). Tin doped indium oxide thin films: Electrical properties. J. Appl. Phys., 83: 2631-2645.

Tauc J (1979). Amorphous and Liquid Semiconductors. Plenum Press, New York, p. 159.

Xue J, Uchida S, Rand BP, Forrest SR (2004). 4.2% efficient organic photovoltaic cells with low series resistances. Appl. Phys. Lett., 84: 3013-3015.